PRE AND POST-BURNING ANALYSIS OF NANO-ALUMINIZED SOLID ROCKET PROPELLANTS

L. Galfetti, L.T. DeLuca, F. Severini, G. Colombo
Politecnico di Milano, SPLab, Milan, Italy

L. Meda, G. Marra
Polimeri Europa, Istituto G. Donegani, Novara, Italy

Nomenclature

a : constant in Vieille burning rate law
n : steady burning rate pressure sensitivity
p : pressure
r_b : steady burning rate
DOA: DiOctilAdipate
EEW: Electrical Explosion of Wires
EM: Electron Microscopy
HTPB: Hydroxyl-Terminated PolyButadiene
IPDI: IsoPhorone-DIsocyanate
MDI: Methyl Disocyanate
PEG: PolyEthylene Glicole
PPG: Polypropylene Glicole
XPS: X-ray Photoelectron Spectroscopy
XRD: X-Ray Diffraction

1. Introduction

Great attention was recently focused on solid propellant formulations containing ultrafine energetic particles, particularly Al nanoparticles, because of advantages such as significant increases in propellant burning rates, shorter ignition delays and shorter agglomerates burning times [1,2]. Nano-particles can enhance the linear burning rate of aluminized solid propellants by 100% or even more. Problems connected with poor mechanical properties and with a higher content of condensed Al_2O_3, which is responsible for specific impulse reduction, limit the use of nano-sized Al propellants and suggest further investigations.

A research program was planned at SP Lab of Politecnico di Milano, in cooperation with Istituto Donegani in Novara, to investigate properties, structure, composition of conventional sized Al powders and nano-sized Al powders (from Russia and U.S.A., coated and uncoated), to test the ballistic properties of AP/HTPB composite propellants manufactured using these powders, and to perform a post-burning analysis of the condensed combustion products. Different series of aluminum powders have been analyzed in a compared characterization: they have different particle size and morphology, due to different preparation procedures. A detailed physical and chemical analysis of the powders is performed using SEM (Scanning Electron Microscopy),

XPS (X-ray Photoelectron Spectroscopy), XRD (X-ray Diffraction).

Emphasis is given in this paper to the condensed combustion products which are investigated by EM, XPS, and XRD to characterize their morphology, size, chemical composition and structure. Significant changes are observed when the currently used micrometric Al powders (30-50 μm nominal size) are replaced by nanometric powders (0.1-0.2 μm) showing that the condensed combustion products feature different oxidation histories.

2. The investigated Aluminum powders

The Aluminum powders investigated in this paper are summarized in Table 1. Both nanometric (or ultra-fine) and micrometric (spheres or flakes) size ranges are investigated. Al_01a is a powder obtained by the EEW technique, while Al_03-d is obtained by a pneumatic mill technique. Aluminum type 05 (spheres of 30 μm) is a standard Al powder traditionally used in solid propellant formulations for space propulsion, while Al type 06 (flakes of 50 μm characteristic dimension) is a cheap commercial product.

Table 1

Nomenclature	Source, production technique, and size
Type 01 Al_01a	*Source: Russia* EEW; uncoated; nominal size: 0.15 μm
Type 03 Al_03-d	*Source: Russia* Pneumatic mill; uncoated; nominal size: 2.5 μm
Type 05 Al_05	*Source: Italy* spherical; nominal size: 30 μm
Type 06 Al_06	*Source: Italy* Flakes; nominal size: 50 μm

3. Solid propellant formulations

The composite propellants tested in this investigation were manufactured with the purpose to contrast the effects of nanometric vs. micrometric Al powders in reducing surface agglomeration and thus promoting single particle combustion. In this respect, a baseline formulation consisting of 68% ammonium perchlorate (AP), 17% HTPB binder, and 15% aluminum (Al) was selected. All propellants of Tables 2 and 3 employ a bimodal AP size distribution: coarse particles (80%) in the range 140-160 μm and fine particles (20%) in the range 70-80 μm. Propellants of Table 4 use a monomodal AP size distribution in the range 140-160 μm. All tested compositions contain 83% mass fraction of solids.

Three different propellant series were tested, for a total of eleven compositions. Series I (see Table 2) is meant to contrast the effects of micrometric Al replaced by the same amount of nanometric Al.

Table 2

AP/HTPB/Al First Propellant Series [AP size: 80% 150 ±10 μm + 20% 75 ± 5 μm] Binder: 17 % [HTPB + DOA + IPDI]			
Propellant	Al powder	Al powder nominal size	Density g/cm^3
P_01a	Al_01a	0.15 μm	1.67
P_03d	Al_03-d	2.5 μm	1.56
P_05	Al_05	30 μm	1.52
P_06	Al_06	50 μm	1.59

Series I includes four Al compositions between the two bracketing formulations P_01a and P_06 respectively consisting of 100% ultra-fine 0.15 μm Al particles and 100% micrometric (50 μm characteristic dimension) Al flakes. The remaining two propellants of Series I (P_03-d and P_05) include 2.5 or 30 μm (coarse) particle sizes.

Table 3

AP/HTPB/Al Second Propellant Series [AP size: 80% 150 ±10 μm + 20% 75 ± 5 μm] Binder: 17 % [HTPB + DOA + IPDI]			
Propellant	Al powder	Al powder nominal size	Density g/cm^3
P_07-B01	80% type 06 20% type 01a	50 μm 0.10 μm	1.63
P_07-B03d	80% type 06 20% type 03-d	50 μm 2.5 μm	1.57

Series II (see Table 3) is meant to assess the effects of bimodal Al distribution, according to the amounts indicated.

The five propellants of Series III (see Table 4) aim to assess the effects of different binders.

Table 4

AP/HTPB/Al Third Propellant Series [AP size: 100% 150 ±10 μm] Aluminum powder: 100 % type 06				
Propellant	Binder			Density g/cm^3
P_06/x1	HTPB	DOA	MDI	1.49
P_06/x2	PEG	DOA	MDI	1.50
P_06/x3	PPG	DOA	MDI	1.72
P_06/x4	PEG	DOA	2-MDI	1.30
P_06/x5	PEG PPG	DOA	MDI	1.55

4. A summary of pre-burning analysis

A pre-burning analysis, mainly concerning the Aluminum powder characterization, has been considered in recent papers of this research group [3,4,5]. For a reason of space only a very short summary is given here.

A variety of EM analyses was used to investigate shape and dimension of the powder grains; for details see [5]. Al_01a powder at a large scale (50K magnification) shows different types of irregular agglomerates, formed by primary spherical particles, whose diameter size is between 50 and 150 nm (Fig. 1). Sample Al_03-d shows a completely spherical morphology (Fig. 2) of monodispersed particles and at higher magnification the absence of a nanometric structure inside spherical particles can be observed. Similar results are obtained for the Al_05 sample (Fig. 3).

XPS profiles allow to investigate atomic composition in a subsurface region, up to a depth of the order of hundreds of nanometers and to quantify the concentrations of main constitutive elements, hydrogen excluded; for details see [5]. Possible contaminations, at a concentration higher than 0.1 at. %, can also be detected.

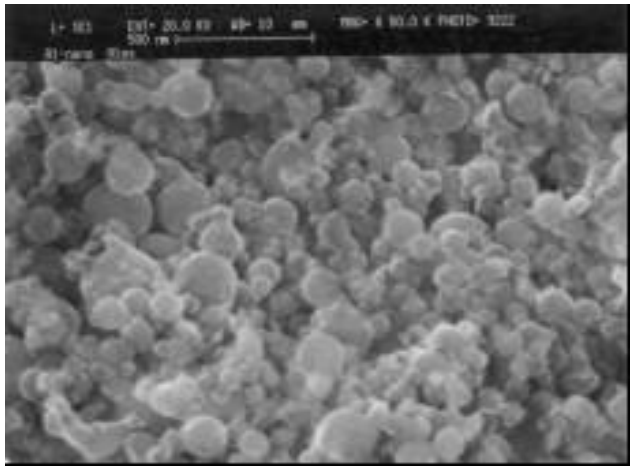

Fig. 1. SEM micrograph of Al_01a powder (magnification: 50 Kx).

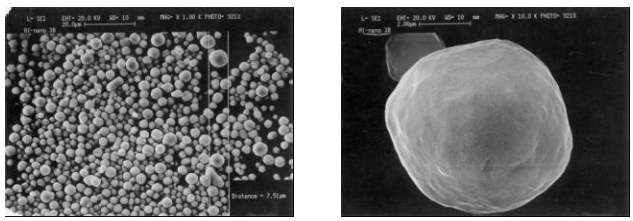

Fig. 2. SEM micrograph of Al_03-d powder (magnification: 1 Kx (left) and 10Kx (right)).

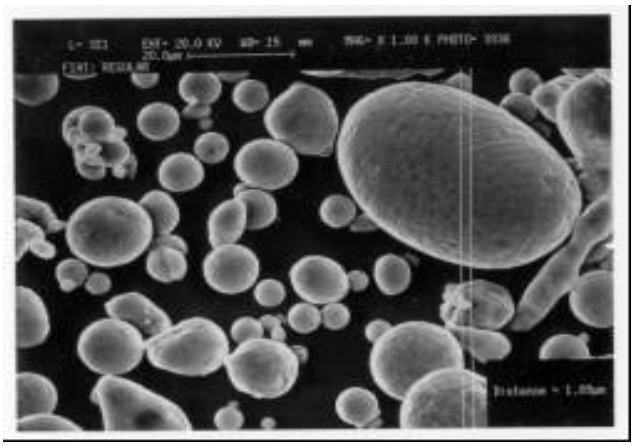

Fig. 3. SEM micrograph of Al_05 powder (magnification: 1 Kx).

These data represent the average on the sampled zone, that usually contains several single particles with the contribution of their native-oxide coatings. In Tab. 5 the Al_{met}/Al_{ox} ratio is reported and its variation with particle diameter is shown.

The chemical depth profile of sample Al_01a is characterized by the presence of three main elements: Al, O, and N (Table 5). Chemical profiles obtained from the series Al_03, prepared by mechanical mixing, never show the presence of nitrogen, because AlN is formed only under severe conditions. The profile of sample Al_05 and also of sample Al_06 are similar to the ones of series Al_03; metal-Al is the prevailing element and the ratio O/Alox tends to reach 1 in bulk.

Table 5

% at	O	Al	N	O/Al_{ox}	Al_{met}/Al_{ox}
Al_01a	33	63	2	1.3	1.6
Al_03d	22	78	-	1.4	3.8
Al_05	12	88	-	0.9	5.6
Al_06	12	86	-	1.4	11.0

The crystalline phases and their relative amounts are obtained by *XRD*; for details about the technique see [5] and [11]. As can be observed in Table 6, the sample prepared by *EEW* contains two crystalline phases: the larger fraction is metallic-aluminum (Al > 90%), with a small fraction of aluminum nitride (AlN < 10%). The crystalline domain sizes (Φ) represent the maximum extension of ordered regions. Generally, this length is lower than particle size, because amorphous material can embed the crystals. Powder Al_01a contains two crystalline phases: metallic-aluminum (Al 96.5%) and aluminum-nitride (AlN 3.5%). Their average crystalline domain lengths (Φ) are 130 nm and 20 nm, respectively. Sample Al_03-d presents an infinite length of crystalline domains, that means they are greater than 500 nm. Sample Al_05 shows 200 nm.

Table 6

Sample		Identified phases	
		Al	AlN
Al_01a	%	96.5	3.5
	Φ (nm)	130	20
Al_03d	%	100	-
	Φ (nm)	∞	-
Al_05	%	100	-
	Φ (nm)	200	-
Al_06	%	100	-
	Φ (nm)	∞	-

A summary of burning analysis

Propellant samples (4.5 x 4.5 x 30 mm) of the formulations under examination were burned in a nitrogen-flushed window bomb in order to measure the steady burning rate. Samples were ignited by a hot Nichrome wire. Pressure was kept constant during the whole combustion process with a feedback pressure control system. Steady burning rates were measured in the range 1-70 bar, using an automated image processing technique from high-speed video recordings. Several samples (at least 3) were used for each experimental point and for each sample several burning rate readings were performed, according to well-established SPLab procedures. Among the several compositions tested, few selected propellants are discussed in this paper. Steady burning rate (Vieille law) of propellants of Tables 2 and 3 are summarized in Table 7.

Table 7

Propellant Short Notation	Vieille burning rate law, $r_b = a\ p^n$	
	a, mm/s	n, (mm/s)/(bar^n)
P_01a	2.42 ± 0.07	0.38 ± 0.01
P_03d	1.46 ± 0.06	0.37 ± 0.01
P_05	1.32 ± 0.03	0.39 ± 0.01
P_06	1.08 ± 0.03	0.42 ± 0.01
P_07-B01	2.04 ± 0.07	0.35 ± 0.01
P_07-B03d	1.27 ± 0.10	0.44 ± 0.03

6. The condensed combustion products analysis

Combustion of metallized solid rocket propellants results in the formation of condensed combustion products (CCP), which have an essential influence on rocket motor performance.

Different techniques are proposed in the literature to collect and analyze the condensed combustion products. Agglomerates are systems made of aluminum and aluminum oxide, formed during the combustion process, whose size is over a defined threshold. Babuk et al. [7] show the influence of the oxidizer particle size on the mass of the agglomerates. Babuk [8] also comments on the effect of binder properties on agglomeration concluding that the binder influence is determined by the content of carbon and easily gasifying elements in the binder itself. Further studies performed by Glotov et al. [9] point out several influences of the binder type on the agglomeration process. They find opposite effects for propellants containing different oxidizers on agglomerates quantities and sizes. Coating Al particles with high-melting metal films (Ni, Cu, Fe) decreases agglomeration; a similar effect can also be reached by using organic substances for coating [10].

Results concerning the technique to collect and analyze the CCP by this group can be found in [11].

6.1 SEM analysis

SEM allows a visual inspection of the combustion residues. The general trend shown by SEM analysis seems to confirm, for the investigated propellants and under the operating conditions used, that agglomeration is poor for coarse Al powder, but consistent for nano-Al powder. A comparison of SEM micrographs for propellants P_01a and P_05, at the pressure of 1 bar and at the same magnification, is shown in Fig. 4 and 5.

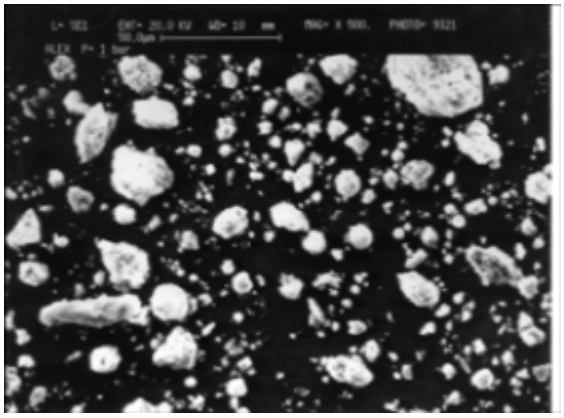

Fig. 4. SEM micrograph of condensed combustion residues of P_01a propellant (magnification: 500x)

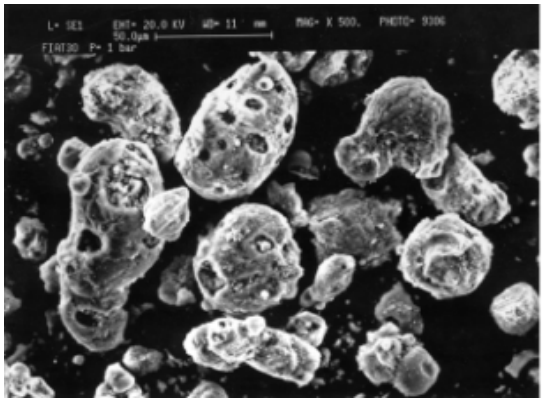

Fig. 5. SEM micrograph of condensed combustion residues of P_05 propellant (magnification: 500x)

6.2. XPS analysis

XPS analysis concerns the surface of the residues, while the bulk composition is better investigated by XRD; for details see [5] and [11]. In spite of these characteristics, XPS allows to obtain interesting results: Tables 8, 9 and 10 show the total amount of atomic species in each state, respectively for propellants of Tables 2, 3 and 4. Carbon comes from pyrolysis processes and is partially oxidized. Al is the total Al, mainly detected as Al oxide, while metal Al contained inside CCP does not appear in the XPS analysis of the residues. Chlorine is probably chlorine from AP decomposition, entrapped in the CCP.

Table 8

	P_01a		P_05	
Press.	1 bar	30 bar	1 bar	30 bar
	% at	% at	% at	% at
O1s	49.7	45.1	46.8	45.7
Al2s	38.2	34.0	30.2	36.2
C1s	10.4	19.4	17.4	16.3
Cl2p	1.4	1.1	2.4	1.3

Table 9

Chem. species	P_07-B01	P_07-B03d
	p = 30 bar	
	% at	% at
O1s	45.8	42.9
Al2p	32.1	30.4
C1s	19.8	24.9
Cl2p	1.5	1.5

Table 10

Chem. species	Propellant (p = 30 bar)				
	P06/x1	P06/x2	P06/x3	P06/x4	P06/x5
	% at	% at	% at	% at	% at
O1s	43.2	39.7	45.8	46.6	37.8
Al2p	30.8	31.3	35.6	35.2	29.8
C1s	25.5	27.8	16.5	17.2	31.5
Cl2p	0.5	0.3	0.7	0.7	0.5

6.3 XRD analysis

XRD spectra were obtained to disclose the crystalline phases and their relative abundance; for details about the technique see [5] and [11]. The results of the X-ray powder analysis relative to the combustion products for propellants P_01a and P_05 are summarized in Table 11. All the powders contain the same inorganic phases, that is γ Al_2O_3, δ*Al_2O_3 , α Al_2O_3 and metallic aluminum (Al°) as shown in Tables 11 and 12. The first two phases are metastable transition aluminas and the third one is the well-known Corundum. At first sight, the aluminum content of residues suggests that the higher pressure favors the metal burning and that the burning performance of propellant P_01 is much better than P_05 one.

Table 11

	P_01a		P_05	
Press.	1 bar	30 bar	1 bar	30 bar
Al^0	3.6	1.5	71.9	9.8
γ Al_2O_3(%)	56.7	57.2	16.7	48.4
δ*Al_2O_3(%)	37.4	37.7	9.0	40.0
α Al_2O_3(%)	2.4	3.6	2.4	1.8

Table 12

	P_07-B01	P_07-B03d
	p = 30 bar	
Al^0	8.4	13.5
γ Al_2O_3(%)	55.5	56.3
δ*Al_2O_3(%)	34.2	29.6
α Al_2O_3(%)	1.9	0.6

Secondly, although the temperatures inside the chamber are well above the value requested to get the α form (≈1400 K), the transition aluminas γ and δ* found in all the samples and their relative abundance means that these temperatures have been experienced by the residues only for very short times. Furthermore, there should be a high temperature gradient between the burning surface of the propellant and the layers below, so that most part of aluminum oxidized is involved in a

temperature range typical of transition aluminas γ and δ* (800 –1200 °C).

Conclusions

To perform a pre-burning analysis of solid rocket propellants, an extensive characterization of micro and nano-sized aluminum powders, using SEM, XPS and XRD techniques was carried out. Powder Al_01a, in comparison with other powders, is a very finely dispersed powder at the nano scale.

Concerning the burning analysis, tests on the propellants considered in this study show that intense Aluminum combustion close to the burning surface, occurring when 0.15 μm is used in place of 30 or 50 μm Al, significantly increases the burning rate. The increased surface area per unit volume greatly contributes to the high reactivity of nano-sized particles.

The post-burning analysis shows the better combustion efficiency of nano-sized aluminized propellants, in comparison with micro-sized, and the important effect of pressure on chemical composition, size and morphology of combustion products.

The important role of the binder nature in agglomeration process has been shown. In particular the use of PPG (see Table 10) allows to obtain significant decreases of unburned aluminum and increases in aluminum oxide among the combustion products. Again, using PPG the carbon content of the residues decreases and their sizes also decrease.

References

[1] Mench, M.M., Yeh, C.L., and Kuo, K.K., "Propellant Burning Rate Enhancement and Thermal Behavior of Ultra-Fine Aluminum Powders (Alex)", Energetic Materials: Production, Processing and Characterization, Proceedings of the 29th International Annual Conference of ICT, 30-1-15, Karlsruhe, Federal Republic of Germany, 1998.

[2] Dokhan, A., Price, E.W., Sigman, R.K., and Seitzman, J.M., "Combustion Mechanism of Bimodal and Ultra-fine Aluminum in AP Solid Propellant", AIAA Paper 2002-4173, 38th AIAA/ASME/SAE/ASEE Joint Propulsion Conference and Exhibit, Indianapolis, IN, July 7-10, 2002.

[3] Olivani, A., Galfetti, L., Severini, F., Colombo, G., Cozzi, F., Lesma, F., and Sgobba, M., "Aluminum Particle Size Influence on Ignition and Combustion of AP/HTPB/Al Solid Rocket Propellants", presented at RTO Specialist's Meeting on Advances in Rocket Propellant Performance, Life and Disposal for Improved System Performance and Reduced Costs, Applied Vehicle Technology Panel (AVT), Aalborg, Denmark, 23-26 September 2002.

[4] Galfetti, L., Severini, F., DeLuca, L.T., and Meda, L., "Nano Propellants for Space Propulsion", Space Propulsion 2004, 4th International Spacecraft Propulsion Conference, Chia Laguna (Cagliari), Italy, 2-9 June 2004. Proceedings SP-555 of Space Propulsion 2004, ESA.

[5] Meda , L., Marra, G.L., Braglia, R., Abis, L., Gallo, R., Severini, F., Galfetti, L., and DeLuca, L.T., "A Wide Characterization of Aluminum Powders for Propellants", Proceedings of the 9-IWCP, Novel Energetic Materials and Applications, November 2004, paper 17.

[6] Babuk, V.A., Vassiliev, V.A., and Sviridov, V.V., "Formation of Condensed Combustion Products at the Burning Surface of Solid Rocket Propellant", Solid Propellant Chemistry, Combustion, and Motor Interior Ballistics, AIAA Progress in Astronautics and Aeronautics, edited by V. Yang, T.B. Brill, W.Z. Ren, Vol. 185, 2000, pp. 749-776.

[7] Babuk, V.A., Vassiliev, V.A., and Malakhov, M.S., "Condensed Combustion Products at the Burning Surface of Aluminized Solid Propellant", *AIAA-JPP*, Vol. 15, No. 6, 1999, pp. 783-793.

[8] Babuk, V.A., Vassiliev, V.A., and Sviridov, V.V., "Propellant Formulation Factors and Metal Agglomeration in Combustion of Aluminized Solid Rocket Propellant", *Combustion Sci. and Tech.*, 2001, pp. 261-289.

[9] Glotov, O.G., Zarko, V.E., Karasev, V.V., and Beckstead, M.W., "Effect of Binder on the Formation and Evolution of Condensed Combustion Product of Metalized Solid Propellants", Proceedings of the 28th International Annual Conference of ICT, Karlsruhe, Germany, 1997.

[10] Risha, G.A., Boyer, E., Wehrman, R.B., and Kuo, K.K., "Performance Comparison of HTPB-Based Solid Fuels Containing Nano-Size Energetic Powder in a Cylindrical Hybrid Rocket Motor", 38th AIAA/ASME/ SAE/ASEE Joint Propulsion Conference and Exhibit, July 2002.

[11] Galfetti, L., Severini, F., DeLuca, L.T., Marra, G.L., Meda, L., and Braglia, R., "Ballistics and Combustion Residues of Aluminized Solid Rocket Propellants", Proceedings of the 9-IWCP, Novel Energetic Materials and Applications, November 2004, paper 18.